Food Sci. Biotechnol. 20(4): 1033-1042 (2011)
DOI 10.1007/s10068-011-0141-3

RESEARCH ARTICLE

Integrity and Cell-monolayer Permeability of Chitosan Nanoparticles in Simulated Gastrointestinal Fluids

Juyoung Lee, Sanghoon Ko, Hanbyul Kim, and Hoonjeong Kwon

Received: 27 February 2011 / Revised: 4 May 2011 / Accepted: 12 May 2011 / Published Online: 31 August 2011

Abstract The objective of this study was to assess the integrity and intestinal permeability of chitosan nanoparticles (CNPs) in simulated gastrointestinal fluids (SGIF). The cell-associated and transported chitosan was quantified and visualized after incubation of the CNPs with Caco-2 cell monolayer with/without SGIF treatment. In order to establish the role of proteins in the SGIF, CNPs were incubated with 4 proteins having different isoelectric points (pI). CNPs incubated with the fluids did not attach to the cell monolayer in contrast to the intact CNPs. Negatively-charged protein formed the complex with CNPs leading to particle size increase, but protected CNPs from disintegration. In contrary, positively-charged protein interacted with cross-linker causing disintegration of CNPs. CNPs incubated with the fluids did not attach to the cell monolayer in contrast to the intact CNPs. The results suggested that the surface charges of CNPs and proteins play a critical role in structural changes of CNPs in biological environment.

Keywords: chitosan nanoparticle, *in vitro* digestion, Caco-2 cell monolayer, particle integrity, surface charge

Juyoung Lee, Hanbyul Kim, Hoonjeong Kwon (✉)
Department of Food and Nutrition, Seoul National University, Seoul 151-742, Korea
Tel: +82-2-880-6835; Fax: +82-2-884-0305
E-mail: hjkwon@snu.ac.kr

Sanghoon Ko
Department of Food Science and Technology, Sejong University, Seoul 143-747, Korea

Hoonjeong Kwon
Research Institute of Human Ecology, Seoul National University, Seoul 151-742, Korea

Introduction

Oral route is most common and non-invasive way to deliver drugs or nutrients into the body. There are some limitations, however, such as the harsh condition in gastrointestinal (GI) tract or poor intestinal absorption, which can in turn, lowers the bioavailability of bioactive materials. Over the past two decades, many researchers have developed various polymeric nanoparticulate systems as a strategy for oral delivery to overcome these limitations and deliver proteins, peptides, vaccines, DNA, and/or nutrients efficiently (1-5). In particular, chitosan, a cationic polysaccharide, has been broadly studied as a carrier material for oral delivery because chitosan is known for non-toxic, biocompatible, and mucoadhesive properties. Nanoparticles composed of chitosan or their derivatives have been examined to enhance permeation of bioactive materials through intestinal epithelium. They were proved to improve intestinal absorption and enhance the therapeutic effects of bioactive materials from *in vitro* (6-10), *ex vivo* (9,10), and *in vivo* studies (11-15) reported by many research groups.

Prior to application of the delivery system into the living organism, the characteristics of the carrier materials as well as the efficiency of the inner target materials are needed to be fully understood. Chitosan is a polymer which is nontoxic when administrated orally, because it is hardly absorbed through the intestinal epithelium (16). However, nano-sized particles would have different characteristics compared with their original form. Indeed, some evidences have shown that chitosan nanoparticles can be able to permeate to the intestinal epithelial cells or tissues themselves while enhancing bioavailability of inner target materials to deliver (6,8-11,15). For this reason, the characteristic and safety of chitosan nanoparticles (CNPs) and those of their original form, soluble chitosan, should be

evaluated separately.

Furthermore, when CNPs are exposed to the biological fluids in a living system prior to the contact to the adsorption site, the therapeutic power or permeation ability of inner target materials and carrier materials are changed consequently (11,17,18). Proteins around nanoparticles are adsorbed to the surface of the CNPs, in turn form the complex called nanoparticle-protein 'corona' (19). Moreover, the CNPs-protein complex is the ultimate form recognized by the cells before absorption (20). Nevertheless, most previous results have been derived from experiences using intact CNPs maintaining their original structure and properties, regardless of the effects of the biological fluids.

Accordingly, the aim of this study was to characterize the CNPs without inner target materials when they are orally applied to the biological fluids. To demonstrate the digestive stability of CNPs, the physical and structural changes of CNPs were evaluated, including mean diameter, ζ potential, and structural integrity in the simulated gastric and intestinal fluids (SGF, SIF, respectively) containing several digestive enzymes. Furthermore, the cell-associated intact CNPs, digested CNPs, and soluble chitosan were quantified respectively using attatched fluorescent dyes and visualized through confocal laser scanning microscope (CLSM). Finally, the effect of protein's isoelectric point (pI) value on the formation of CNPs-protein complex was examined.

Materials and Methods

Materials Chitosan was offered from Keumho Chemical Products Co., Ltd. (Seoul, Korea). Viscosity (in 0.5% acetic acid, 20°C) of chitosan was 4.0 cp, degree of deacetylation was 90.0%, and molecular weight (Mw) was 50 kDa. Fluorescein isothiocyanate (FITC), tripolyphosphate (TPP), paraformaldehyde (PFA), and trypan blue were purchased from Sigma-Aldrich (St. Louis, MO, USA). Porcine originated pepsin, lipase, and pancreatin, chicken egg white originated lysozyme, and *Candida rugosa* originated lipase were also purchased from Sigma-Aldrich, and bovine serum albumin (BSA) was from Amresco Inc. (Solon, OH, USA). Whatman filter paper no.1 (Whatman, Maidstone, Kent, UK), Amicon® ultra centrifuge filter (Millipore, Bedford, MA, USA), 12-well transwell plate (Corning, Corning, NY, USA), 8-well Lab-Tek chamber slides (Nunc, Roskilde, Denmark), sodium dodecyl sulfate (SDS) (Roche, Mannheim, Germany), Pierce® BCA protein assay kit (Pierce, Rockford, IL, USA), and mounting solution (Biomeda, Foster City, CA, USA) were purchased. Dulbecco's modified eagle medium (DMEM), fetal bovine serum (FBS), sodium pyruvate solution, antibiotic-antimycotic solution, MEM non-essential amino acids solution, and phosphate buffered saline (PBS) were purchased from Gibco (Gaithersburg, MD, USA), and Hank's buffered salt solution (HBSS) and sodium bicarbonate from Sigma-Aldrich. Hydrogen chloride, sodium hydroxide, methanol, and acetic acid were purchased from Samchun Chemical Co. (Pyungtaek, Korea). Size and ζ potential analyzer (Delsa nano C; Beckman Coulter, Fullerton, CA, USA), fluorescence multiplate reader (Victor3; Perkin-Elmer, Torrance, CA, USA), Millicell®-ERS (Millipore), and CLSM (Carl Zeiss-LSM510; Carl Zeiss, Jena, Germany) were used for analyses.

Preparation of FITC-labeled chitosan nanoparticles One g of chitosan was dissolved in 100 mL of 0.1 M acetic acid. The solution was filtrated through filter paper. A100 mL of methanol, followed by 50 mL of FITC in methanol (1 mg/mL), was slowly added to the chitosan solution with stirring. The D-glucosamine residues/FITC ratio was controlled to about 58:1. The mixture was kept in continuous stirring in the dark at ambient temperature for 3 h. The FITC-labeled chitosan (fChi) was precipitated by adding 2 N NaOH and then centrifuged at 30,000×g for 15 min. The pellet was re-dissolved in 0.1 M acetic acid and washed with 70%(v/v, with water) methanol, and then precipitated again. This washing step was repeated until fluorescence was not detected in the supernatant. Fully washed fChi was freeze-dried and stored at −80°C (21-24). Dried fChi was washed again with 70% methanol, and after complete washing, fChi was freeze-dried again and stored at −80°C until use.

FITC-labeled chitosan nanoparticles (fCNPs) were prepared by the ionotropic gelation with TPP as cross-linker. While stirring at 830 rpm, 0.7 mg/mL TPP solution was added dropwise to 0.05% fChi solution in 1%(v/v) acetic acid until volume ratio reached 1:3. The mixture was kept stirring for 2 h at ambient temperature (25). Characterization of fCNPs was conducted immediately with the size and ζ potential analyzer. fCNPs were freshly prepared before conducting each experiment.

Assessment of the digestive stability of chitosan nanoparticles in simulated gastrointestinal environment To assess the structural changes of CNPs in the GI tract, the modified *in vitro* digestion system first described by Garret *et al*. (23) was employed (24). Briefly, for gastric phase, CNPs suspension was acidified to pH 2.0 with 6 N HCl, and then pepsin (8,26) obtained from porcine gastric mucosa was added into the tube to the final concentration of 0.91 mg/mL. Suspension was incubated at 37°C for 1 h in shaking water bath at 150 rpm. Suspension pH was adjusted to 5.3 with 0.9 M sodium bicarbonate solution after 1 h incubation, and intestinal enzyme solutions (bile extract, lysozyme, pancreatin, and porcine lipase) were

added for simulating small intestinal phase. The final concentrations of each enzyme were adjusted to 1.23, 0.09, 0.21, and 0.10 mg/mL, respectively. Suspension pH was raised up to 7.0 and incubated again at 37°C for 2 h with shaking. The enzyme-untreated (enz.-) suspensions paired with each phase were also prepared to examine the effect of pH.

The size distribution, ζ potential value, and degree of disintegration (DD) of CNPs were measured at 3 points: before incubation, after gastric incubation, and after intestinal incubation. The first 2 parameters were measured using the size and ζ potential analyzer. DD of CNPs was measured by quantification of free soluble fChi in supernatant disintegrated from fCNPs through ultracentrifugation of fCNPs suspension at 100,000×g for 50 min. Before ultracentrifugation, pH of suspension was adjusted to 2.0 to dissolve free fChi in supernatant. The amount of free fChi was determined by measuring the fluorescence intensity (λ_{ex}=485 nm, λ_{emi}=530 nm) against standard solution of fChi (8,26) and all solution pHs were adjusted to 5.9 using 2 N sodium acetate solution before measurement of fluorescence intensity. To quantify enzymatically digested short-chain fChi, ultrafiltration was conducted: After ultracentrifugation, the supernatant of CNPs suspension was added to the Amicon ultra filter device (Mw cut off=10 kDa), and the device was centrifuged at 14,000×g for 15 min. The fluorescence intensity of filtered solution was measured.

Caco-2 cell culture Caco-2 cells were cultured and maintained in high glucose (4.5 g/L) DMEM, supplemented with 10%(v/v) FBS, 584 mg/L L-glutamine, 0.1 mM MEM non-essential amino acids, and 1% antibiotic-antimycotic solution. Cells were expanded and cultivated in a cell culture incubator set at 37°C, 5% CO_2, and 95% relative humidity. Caco-2 cell monolayer is usually reached confluence after 5±1 days. After reaching 80% confluence, cells were digested by using 0.25% trypsin containing 1 mM EDTA for subculture (6).

Transport study Caco-2 cells were seeded on polycarbonate 12-well transwell plate at a density of 1×10^5 cells/cm^2 and used for transport experiment on 19 days after seeding. The integrity of the cell monolayer was assessed before the study by measurement of transepithelial electrical resistance (TEER) using a Millicell®-ERS. TEER values of cultured monolayer were in the range of 500-700 Ω·cm^2 (11). Transport study was initiated by pre-incubation of Caco-2 cell monolayer with transport buffer, pre-warmed HBSS at 37°C supplemented with 4.5 g/L glucose added into both insert (0.5 mL) and plate well (1.5 mL) compartments for 30 min. Samples were prepared as follows: Digested fCNPs and digested fChi were prepared as described for *in vitro* digestion and undigested fCNPs were also prepared for the comparison. Final concentration of these test samples was 0.3 mg/mL and final pH of all samples was 7.0. All samples were diluted with transport buffer at a ratio of 3:1 and 0.5 mL of each diluted sample was added into surface of the cells on insert after the removal of pre-incubation buffer. The transwell plate was remained in the cell culture incubator for 2 h, and then the transport experiment was terminated by washing the cell monolayer thrice with ice-cold HBSS. Cell monolayer on the insert was lysed with lysis solution, 300 μL of 5% SDS/HBSS, pH 6.9, for 45 min on the ice. Both cell lysate in the insert and transport buffer in the plate well compartment were collected and the fluorescence intensities were measured immediately. Standards for each solution were separately prepared by diluting cell lysate and transport buffer containing fCNPs. Protein assay was conducted to normalize fluorescence intensity of cell lysate using PierceR BCA protein assay kit. Each experiment was performed in triplicate (6,15,27,28).

Visualization of Caco-2 cell monolayer by confocal laser scanning microscopy (CLSM) Caco-2 cells were seeded onto 8-well Lab-Tek II chamber slides at a density of 1×10^5 cells/cm^2 and cultured in 0.5 mL of DMEM at 37°C in the incubator. After 19 days of culture, the cell monolayer was washed using pre-warmed PBS and treated with samples prepared as follows: 0.3 mL of digested fCNPs (pH 7.0), digested fChi (pH 7.0), undigested fCNPs (pH 6.6), and undigested fCNPs (pH 7.0) with the final concentration of 0.225 mg/mL. Each treatment was duplicated. After 2 h incubation with each sample, 1-well of each paired well was treated with 30 μL of 0.4% trypan blue for 1 min. All samples were removed and cell monolayer was washed twice with PBS, then fixed in 0.2 mL of 4% PFA for 4 h, and mounted with Gel/Mount medium for 1 h. The specimens were kept overnight in the dark and were examined under an inverted confocal microscope equipped with a LSM 5 image browser (8,21,26).

Assessment of the structural stability of chitosan nanoparticles with proteins Four proteins which have different pI values were chosen as follows: lipase from *C. rugosa*, pI<2.0; pepsin, pI=3.0; BSA, pI=4.7; and lysozyme, pI=11. The set of tubes containing 1 mL of fCNPs suspension was divided into 4 different pH groups of 2.0, 3.3, 4.7, and 7.0. Each pH group was subdivided into 4 protein groups: 40 μL of 20% BSA, 20% pepsin, 10% lysozyme, and 2% lipase solution, respectively. These tubes were incubated for 1 h at 37°C in a shaking water bath with 150 rpm. The size distribution, ζ potential, and DD of CNPs-protein complexes were measured after the incubation as described earlier. Same experiments were

conducted for protein solutions without fCNPs and for fCNPs suspension without proteins for comparison. All treatments were performed in triplicate.

Statistical analysis Results are expressed as means± standard deviation (SD). Data were analyzed by two-tailed Student's *t*-test and one-way analysis of variance (ANOVA) followed by Tukey's multiple range test (SPSS 12.0, SPSS Inc., Chicago, IL, USA). Differences were considered to be statistically significant when the *p*-values were less than 0.05.

Results and Discussion

Physical characterization of fCNPs The characteristics of the obtained fCNPs were as follows: mean diameter of 115.1±16.4 nm, polydispersity index of 0.429±0.136, ζ potential of +39.36±2.79 mV, and the final pH of the fCNPs suspension of 3.3.

Exposed to the conditions of GI tract, the physical characteristics and integrity of the CNPs were not maintained because CNPs are susceptible to pH and interact with proteins. The results showed that in the gastric phase (pH 2.0), the mean diameter of enzyme-treated (enz.+) CNPs increased up to 483.7±46.6 nm while that of enz.- CNPs remained almost same mean diameter, 135.2± 35.6 nm (Fig. 1A). From this result, the increase of the particle size was thought to be caused by the interaction with pepsin in SGF. The structure of CNPs at pH 2.0 was reported to be fairly stable than at lower pH (15). On the other hand, in the intestinal phase, CNPs tended to be precipitated due to higher pH (pH 7.0) than pKa value of chitosan, which ranges from 6.2 to 6.8 (29). Regardless of enzyme treatment, the size of aggregated particles more increased in the neutral environment (pH 7.0) than in gastric phase, reaching to micron scale. But with enzymes, the size increased to a lesser extent.

The change of ζ potential was negatively correlated with that of mean diameter. As shown in Fig. 1B, ζ potential of enz.+ CNPs was significantly low compared to that of enz.- CNPs in the gastric phase. It suggests that positively-charged pepsin (pI=3.0) was adsorbed onto the surface of CNPs. When protein is adsorbed onto the surface of electrically charged particles, electrostatic interaction can be considered as a major interaction force between different charges. However, protein adsorption to same charged particles was also observed, though the extent was smaller than to different charged particles (30,31). It could be inferred that other forces between the same charged surfaces such as hydrogen bonding and hydrophobic interaction, seemed to be involved in the adsorption of slight positively-charged pepsin to the CNPs. On the other hand, the ζ potential of CNPs in the intestinal phase was nearly zero in both enz.- and enz.+ cases, and the values were –3.52±0.80 and –4.05±1.17 mV, respectively, suggesting complete precipitation.

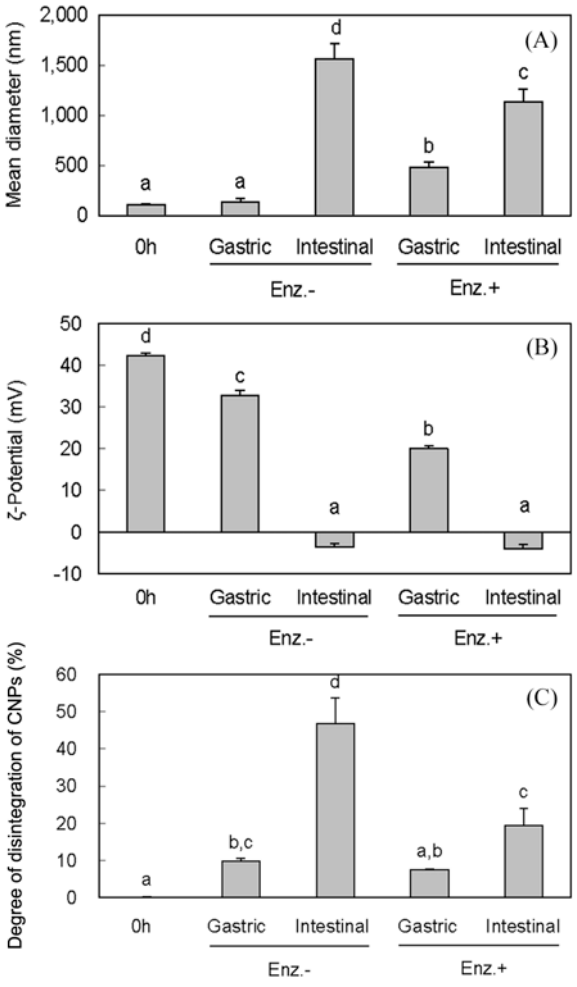

Fig. 1. Changes of the mean diameter (A), ζ potential of CNPs, (B), and the % of free fChi (C) in SGF and SIF (enz.-: CNPs untreated digestive enzymes; enz.+: CNPs treated digestive enzymes). Data points represent mean±SD (n=3); Means with different superscripts (a-d) on the bar are significantly different from each other at p<0.05 as determined by Tukey's multiple range test.

At pH 2.0, free soluble fChi, which is disintegrated from fCNPs, fully dissolves into the supernatant and will not be precipitated by ultracentrifugation. So to quantify the amount of disintegrated chitosan from fCNPs, fluorescence intensity of supernatant was measured after ultracentrifugation of fCNPs suspension at pH 2.0. DD of fCNPs calculated as a percentage against fCNPs concentration of firstly prepared suspension (Fig. 1C).

DD of fCNPs was less than 10% in gastric phase. However, in the intestinal phase, DD of enz.+ fCNPs was 19.5% and that of enz.- fCNPs reached up to 46.8%. The results corresponds to the reports that over 20% of insulin

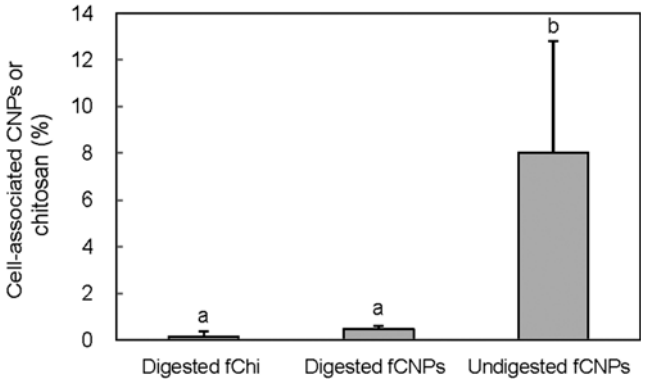

Fig. 2. Percentage of fCNPs or fChi associated with Caco-2 cell monolayer after 2 h incubation at pH 7.0 (mean±SD, *n*=3). Means with different superscripts (a,b) on the bar are significantly different from each other at $p<0.05$ as determined by Tukey's multiple range test.

encapsulated in CNPs was released during 1 h at pH 4.0, and over 80% was released during 2 h at pH 7.4 (11,13). The release of inner target materials (e.g., insulin) may have followed the disintegration of CNPs at each condition. Because free soluble fChi was also precipitated during centrifugation when it forms the complex with proteins, the direct comparison between enz.- and enz.+ cases seems to be meaningless. Nevertheless, Fig. 1C clearly demonstrates the effect of pH on the structural integrity of CNPs.

At the end of incubation for *in vitro* digestion, ultrafiltration for supernatant was conducted with 10 kDa of Mw cut off device to quantify enzymatically hydrolyzed chitosan. Lysozyme, known to hydrolyze chitosan (32) and be secreted by the paneth cells of intestine (33-35), was added to the SIF. If fCNPs or disintegrated fChi were hydrolyzed by enzymes, specifically lysozyme, digested short-chain chitosan would be detected in the filtrate (Mw of chitosan used in this study was 50 kDa). However, insignificant amount was detected, suggesting that the enzymatic digestion of fCNPs in the GI tract could be ignored (data not shown). Ma *et al*. (36) demonstrated that chitosanase and lysozyme did not increase both rate and extent of encapsulated insulin release from CNPs. However, there are not many reports investigating the digestion of CNPs because the major interest is efficient delivery of inner target material in most researches.

Caco-2 cell monolayer permeation study CNPs have been demonstrated to be transported or attached to the intestinal epithelium by cellular uptake, paracellular transport, or by binding to the surface of epithelium. If, however, the features of CNPs are changed by SGF and/or SIF before they contact to the epithelium, the cell-associating ability is also expected to be changed. To verify the effect of these fluids, the amount of cell-associated digested fChi, digested fCNPs, and undigested fCNPs were quantified using Caco-2 cell monolayer. Digested fChi was tested to identify the differences between fChi and fCNPs in an aspect of the cell-associating ability. The amount of cell-associated samples was expressed as a percentage against initial amount fCNPs or fChi treated to the Caco-2 cell monolayer (Fig. 2).

After 2 h incubation, 0.47±0.13% of digested fCNPs was associated with the cells, and there is no significant difference between digested fChi and digested fCNPs. With digestive enzymes and neutral pH, CNPs were not much different from soluble chitosan in an ability to associate to Caco-2 cell monolayer. On the contrary, undigested fCNPs, of which pH was adjusted to 7.0 right before treatment, was relatively well associated within the cell, 8.02±4.78%. From the reported studies, soluble chitosan is known to act as permeation enhancer for hydrophilic bioactive materials through paracellular transport, and be not transported itself into Caco-2 cells after adhesion onto the cell surface. On the other hand, CNPs have been demonstrated that they are likely to be transported into the inner space of Caco-2 cells by transcellular transport pathway (6, 37). The method used in this study was not able to distinguish fluorescence intensity inside the cells from that on the cell surface. Despite, the result indicates that digested CNPs could not be effectively taken up by Caco-2 cells compared to undigested CNPs because its intact form was not maintained in the gastrointestinal environment.

After the transport study, the transport buffer in the plate well compartment of trans-well plate was collected as well as apical side and fluorescence intensity was measured for quantification of transported fCNPs or free fChi through the cell monolayer. But there was no apparent transport of CNPs or free chitosan (data not shown). Lin *et al*. (11) showed that nanoparticles shelled with chitosan open tight junction between adjacent cells at pH 6.6 by reorganizing tight junction protein ZO-1. It seems that the opened tight junction may offer a possibility that CNPs are transported to the basolateral space of the cell layer via paracellular pathway. However, the current result suggested that CNPs orally administered as a carrier materials may be difficult to be transported to the circulate system.

Visualization of Caco-2 cell monolayer by CLSM CLSM visualization was conducted to confirm the results of Caco-2 cell monolayer transport study, and to visualize the cellular site associated with fluorescence-labeled samples without disrupting cell structure. Weak fluorescence intensity was observed in the cell monolayer incubated with undigested fCNPs at pH 7.0 (Fig. 3A). The fluorescence intensity was observed more clearly when cell monolayer was treated with undigested fCNPs at pH 6.6 (Fig. 3B) at which the structure of fCNPs are better

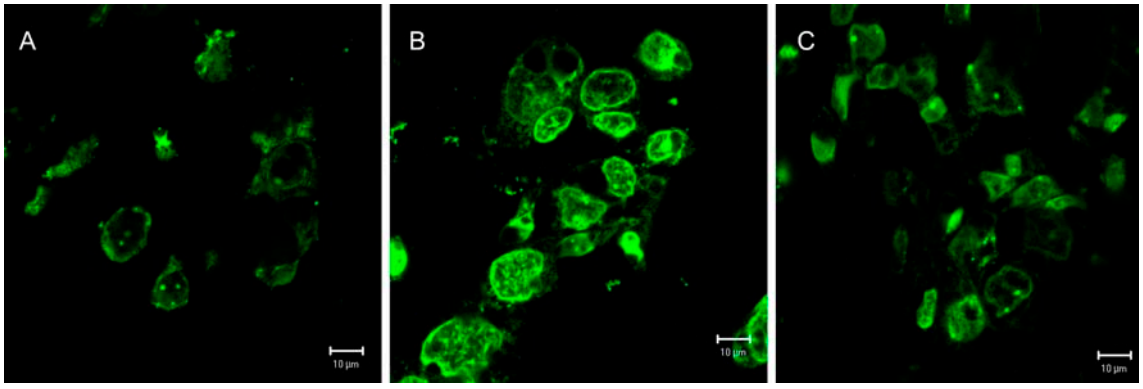

Fig. 3. CLSM images of Caco-2 cell monolayer incubated for 1 h with undigested fCNPs of which pH was adjusted to 7.0 (A), 6.6 (B), and 6.6 followed with addition of trypan blue (C).

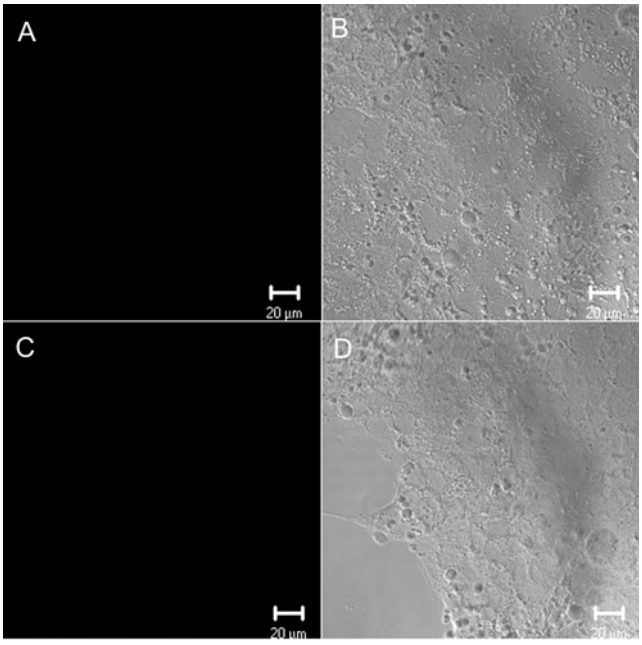

Fig. 4. CLSM images of Caco-2 cell monolayer treated with digested fCNPs (A, fluorescent; B, optical) and digested fChi (C, fluorescent; D, optical).

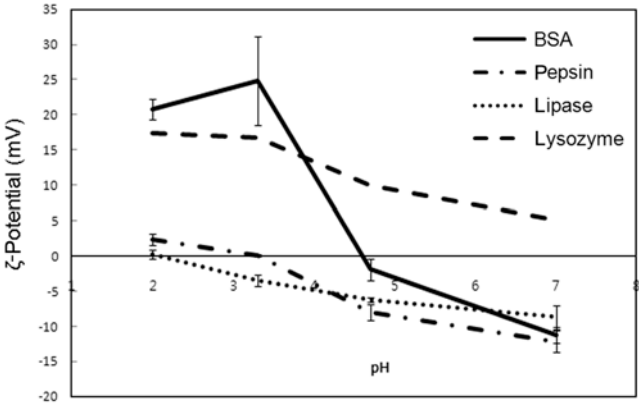

Fig. 5. Changes of ζ potential of protein solutions (BSA, pepsin, lipase, and lysozyme) at various pH conditions (mean±SD, *n*=3).

remained than at 7.0. It corresponds with the results from other studies showing the pH-sensitive transporting ability of CNPs (11,15). The CLSM images showed that the cell-associated CNPs were mainly located in the cell membranes compared with the inner cellular matrix. When the Caco-2 cell monolayer was incubated with digested fChi and digested fCNPs at pH 7.0, no fluorescence was detected inside the cells (Fig. 4). Jia *et al*. (6) and Huang *et al*. (26) already demonstrated that the transcellular transportation is improved when soluble chitosan is transformed into nanoparticles. From this result, it could be confirmed that digested CNPs were not much different from soluble chitosan in the aspect of cellular uptake.

At pH 6.6, trypan blue was added to quench fluorescence intensity from dead cells. After post-treatment of trypan blue, fluorescence intensity still detected in the cells indicating that the cellular uptake of undigested fCNPs was not accompanied by cell death (Fig. 3C). Chitosan, a polycation, could interacts with the cell membrane and cause cell damage consequently. However, the cytotoxic effect of chitosan or CNPs could be disregarded because viability of Caco-2 cell was observed as near 90% when they are treated with 0.3 mg/mL soluble chitosan or CNPs, the concentration used in this study (6).

Assessment of the structural stability of chitosan nanoparticles with proteins The pI of used proteins were roughly verified by measuring the ζ potential of protein solutions (Fig. 5). The measured pI of BSA, pepsin, and lipase were close to 4.6, 3.3, and 2.0, respectively. The pI of lysozyme was not confirmed in this study, but the curve implies that it might be higher than pH 7.0 at least, that is, lysozyme is positively charged at all pH conditions chosen in this study. The pI of lysozyme was found as pH 11 from literature (38), and Rezwan *et al*. (31) reported it as pH 9.5 identified by measuring pH-dependent change of ζ potential of lysozyme.

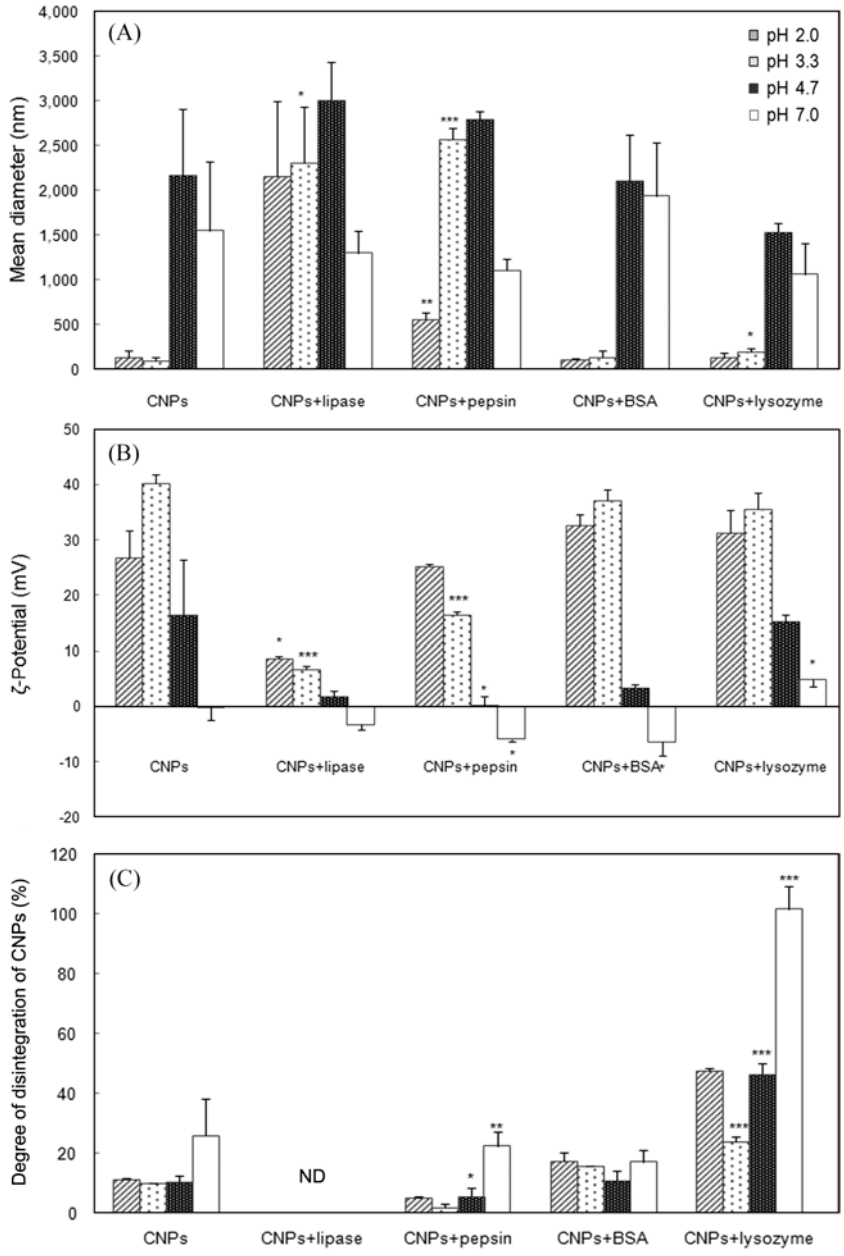

Fig. 6. Changes of mean diameter (A), ζ potential of CNPs-protein complexes (B), and % of free fChi in CNPs suspension (C) after 1 h incubation with proteins (BSA, pepsin, lipase, and lysozyme) at various pH (mean±SD, *n*=3). *$0.05 \geq p > 0.01$; **$0.01 \geq p > 0.001$; and ***$p < 0.001$ were determined by Student's *t*-test; ND, not detected. Each comparison was conducted with CNPs at the same pH condition for A and B. For C, comparison was conducted with different pH condition in same protein-treated group.

CNPs suspended stably at pH 2.0 and 3.0, but the mean diameter of CNPs-lipase and CNPs-pepsin complexes increased up to micron-scale and precipitation was observed at those pH conditions (Fig. 6A). On the other hand, CNPs-BSA and CNPs-lysozyme complexes remained original mean diameter at pH 2.0 and 3.3 (Fig. 6A). At those relatively low pH, BSA and lysozyme were positively charged, but ζ potential of lipase and pepsin were nearly zero or slightly negative (Fig. 5). The mean diameter of CNPs significantly increased with protein at pH condition above pI of each protein (protein is negatively charged), but at below pI value (protein is positively charged), the mean diameter of CNPs were not affected considerably.

The ζ potential of CNPs-protein complexes reflects the surface charge of proteins as well as of CNPs (Fig. 6B). Negatively-charged proteins significantly reduced the ζ potential of CNPs as the data of CNPs-lipase, CNPs-pepsin, and CNPs-BSA at pH 2.0, 3.3, and 4.7, respectively shown. On the other hand, positively-charged proteins, specifically pepsin at pH 2.0, BSA at pH 2.0 and 3.3, and lysozyme at all ranges of pH except at pH 7.0, did hardly change the ζ potential. At pH 7.0, the ζ potential of CNPs

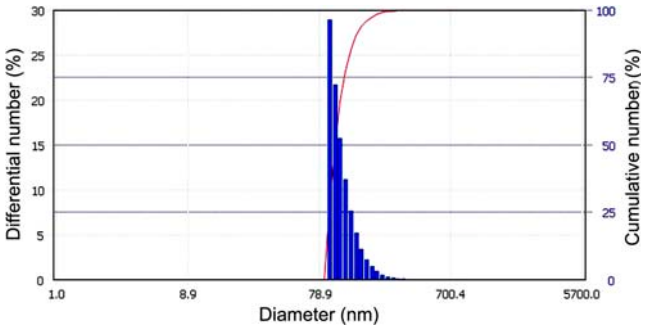

Fig. 7. Size distribution of prepared CNPs represented by number distribution.

was neutral, so that of all complexes represented only protein's ζ potential values.

Interestingly, the clear difference can be noticed between CNPs-lipase and CNPs-lysozyme in terms of mean diameter and ζ potential. Lipase, negatively-charged at all pH used in this study, increased mean diameter of CNPs. The decrease of ζ potential of CNPs-lipase suggests that lipase adsorbs to the surface of CNPs leading aggregation and precipitation of the complex. On the other hand, lysozyme, positively charged at all pH conditions, did not affect the size and ζ potential of CNPs.

Electrostatic interaction govern protein adsorption for the cases where the protein and the particles surface are very hydrophilic (31). Indeed, it could be inferred from current data that surface of CNPs is regarded as hydrophilic at below pH 7.0, repulsive interaction would prevent the adsorption of positively-charged proteins, for instance lysozyme, onto CNPs. It is also noticeable that proteins are relatively well adsorbed onto CNPs and decreased ζ potential of complexes at pI. For less hydrophilic surface, the hydrophobic or hydrogen bonding could be dominant than electrostatic interaction (31,39). So these interactions seem to act on the adsorption of proteins at their pI point.

Unlike mean diameter and ζ potential, positively-charged proteins inflicted more severely on the disintegration of CNPs than negatively-charged proteins. Figure 6C shows that the disintegration pattern of fCNPs and that of fCNPs-pepsin are similar. However, when compared with the case of CNPs alone, BSA caused more disintegration of CNPs at pH 2.0-4.7, at which it is positively charged, than at pH 7.0. Lysozyme increased the amount of free soluble chitosan liberated from fCNPs considerably at all applied pH conditions. From the results, it can be deduced that the positively-charged proteins accelerate the disintegration of CNPs by competing TPP with chitosan. It could also be noticed that Mw of lysozyme is the smallest among that of used proteins (Table 1). Mw or size of proteins might be key factor on disintegration of CNPs in the aspect of accessibility into the interior of CNPs. The dimensions of lysozyme, 3×3×3 nm^3 (31), is apparently small enough to access to the inner space of around 100 nm sized CNPs. When the surface charge of CNPs is neutral, this effect would become stronger as the repulsive force is weakened between same positive charges.

Except fCNPs-BSA complex, CNPs were best remaining integrated at pH 3.3 (Fig. 6C). It might be due to that pH 3.3 is original condition when CNPs are prepared, that is, CNPs were most stable at pH 3.3. On the other hand, in all cases, the largest amount of free soluble chitosan was liberated at pH 7.0 after incubation with proteins.

After the incubation with each protein, the CNPs-protein mixture was centrifuged to obtain supernatant including free soluble chitosan. As mentioned earlier, when the mixture is centrifuged, fCNPs and free soluble fChi tended to precipitate together due to proteins, and the degree of precipitation are different depending on the kind of proteins. For example, most free fChi was precipitated by lipase, so the free fChi left in the supernatant was hardly detectable. On the other hand, when the CNPs-lysozyme mixture was centrifuged, little precipitation of free fChi was observed. That made the direct comparison of the amount of free fChi among the supernatant impossible. Nevertheless, the effect of different pH conditions on the disintegration of CNPs is worth considering when CNPs are incubated with same protein.

To sum up the results of this section, it is suggested that when CNPs-protein complex has ζ potential value below about +15 mV, the mean diameter of complex is likely to increase up to over 1,500 nm. And the complex having these values tended to be severely aggregated and precipitated. The physical characteristics of CNPs were dramatically changed with negatively-charged proteins while positively-charged protein caused the disintegration of nanoparticles. Protein is expected to have repulsive effect to CNPs at pH below its pI value where it is positively charged. But

Table 1. Source, molecular weight (Mw), and isoelectric point (pI) of proteins used in the experiment

	Lipase	Pepsin	BSA	Lysozyme
Source	*C. rugosa*	Porcine gastric mucosa	Bovine serum	Chicken egg white
Mw[1)] (Da)	67,000	35,000	66,462[2)]	14,700
pI[3)]	ca. 2.0	ca. 3.3	ca. 4.6	>7.0

[1)]Offered by companies, except BSA
[2)]Ref. 38
[3)]Estimated from Fig. 5

positively-charged protein is likely to compete for the negatively-charged TPP causing structural disintegration of CNPs by disrupting the cross-link between chitosan and TPP. Competitive effect of protein is likely to become greater when CNPs are almost neutral at pH 7.0. However, at pH above the pI value, proteins would be well adsorbed onto the surface of CNPs increasing size of CNPs-protein complex, but protecting against disintegration of positively-charged CNPs. In contrast, neutral CNPs seemed not to be much affected by negatively-charged proteins.

In conclusion, it was demonstrated in this study that the selected digestive enzymes in the GI tract showed insignificant enzymatic effect on CNPs. However, they can interact with CNPs leading to the physicochemical characteristics and integrity of the particles. CNPs are disintegrated within the SGF and SIF, and cannot be transported across the intestinal cells or associated with Caco-2 cell monolayer unlike intact particles. From this result, CNPs would be expected to behave as soluble chitosan molecule in GI tract. Moreover, the surface charge of CNPs and proteins would be mainly involved in the interaction between them when they form the CNPs-protein complex. In the future studies, the effect of the biological fluids should be considered when evaluate the efficacy or safety of nanoparticles composed of other materials.

References

1. Desai KGH, Park HJ. Recent developments in microencapsulation of food ingredients. Dry. Technol. 23: 1361-1394 (2005)
2. Flanagan J, Singh H. Microemulsions: A potential delivery system for bioactives in food. Crit. Rev. Food Sci. 46: 221-237 (2006)
3. Müller G. Oral delivery of protein drugs: Driver for personalized medicine. Curr. Issues Mol. Biol. 13: 13-24 (2010)
4. Rieux A, Fievez V, Garinot M, Schneider YJ, Prat V. Nanoparticles as potential oral delivery systems of proteins and vaccines: A mechanistic approach. J. Control. Release 116: 1-27 (2006)
5. Shahiwala A, Vyas TK, Amiji MM. Nanocarriers for systemic and mucosal vaccine delivery. Recent Pat. Drug Deliv. Formul. 1: 1-9 (2007)
6. Jia X, Chen X, Xu Y, Han X, Xu Z. Tracing transport of chitosan nanoparticles and molecules in Caco-2 cells by fluorescent labeling. Carbohyd. Polym. 78: 323-329 (2009)
7. Lin YH, Chung CK, Chen CT, Liang HF, Chen SC, Sung HW. Preparation of nanoparticles composed of chitosan/poly-γ-glutamic acid and evaluation of their permeability through Caco-2 cells. Biomacromolecules 6: 1104-1112 (2005)
8. Ma Z, Lim LY. Uptake of chitosan and associated insulin in Caco-2 cell monolayers: A comparison between chitosan molecules and chitosan nanoparticles. Pharm. Res. 20: 1812-1819 (2003)
9. Sandri G, Bonferoni MC, Rossi S, Ferrari F, Gibin S, Zambito Y, Colo GD, Caramella C. Nanoparticles based on *N*-trimethylchitosan: Evaluation of absorption properties using *in vitro* (Caco-2 cells) and *ex vivo* (excised rat jejunum) models. Eur. J. Pharm. Biopharm. 65: 68-77 (2007)
10. Yin L, Ding J, He C, Cui L, Tang C, Yin C. Drug permeability and mucoadhesion properties of thiolated trimethyl chitosan nanoparticles in oral insulin delivery. Biomaterials 30: 5691-5700 (2009)
11. Lin YH, Mi FL, Chen CT, Chang WC, Peng SF, Liang HF, Sung HW. Preparation and characterization of nanoparticles shelled with chitosan for oral insulin delivery. Biomacromolecules 8: 146-152 (2007)
12. Ma Z, Lim TM, Lim LY. Pharmacological activity of peroral chitosan-insulin nanoparticles in diabetic rats. Int. J. Pharm. 293: 271-280 (2005)
13. Pan Y, Li YJ, Zhao HY, Zheng JM, Xu H, Wei G, Hao JS, Cui FD. Bioadhesive polysaccharide in protein delivery system: Chitosan nanoparticles improve the intestinal absorption of insulin *in vivo*. Int. J. Pharm. 249: 139-147 (2002)
14. Sarmento B, Ribeiro A, Veiga F, Sampaio P, Neufeld R, Ferreira D. Alginate/chitosan nanoparticles are effective for oral insulin delivery. Pharm. Res. 24: 2198-2206 (2007)
15. Sonaje K, Lin YH, Juang JH, Wey SP, Chen CT, Sung HW. *In vivo* evaluation of safety and efficacy of self-assembled nanoparticles for oral insulin delivery. Biomaterials 30: 2329-2339 (2009)
16. Hirano S, Seino H, Akiyama Y, Nonaka I. Chitosan: A bibocompatible material for oral and intravenous administrations. pp. 283-290. In: Progress in Biomedical Polymers. Gebelein CG, Dunn RL (eds). Plenum Press, New York, NY, USA (1990)
17. Jintapattanakit A, Junyaprasert VB, Mao S, Sitterberg J, Bakowsky U, Kissel T. Peroral delivery of insulin using chitosan derivatives: A comparative study of polyelectrolyte nanocomplexes and nanoparticles. Int. J. Pharm. 342: 240-249 (2007)
18. Nimesh S, Thibault MM, Lavertu M, Buschmann MD. Enhanced gene delivery mediated by low molecular weight chitosan/DNA complexes: Effect of pH and serum. Mol. Biotechnol. 46: 182-196 (2010)
19. Lynch I, Dawson KA. Protein-nanoparticle interactions. Nanotoday 3: 40-47 (2008)
20. Lynch I, Salvati A, Dawson KA. Protein-nanoparticle interactions: What does the cell see? Nat. Nanotechnol. 4: 546-547 (2009)
21. Huang M, Khor E, Lim LY. Uptake and cytotoxicity of chitosan molecules and nanoparticles: Effects of molecular weight and degree of deacetylation. Pharm. Res. 21: 344-353 (2004)
22. Amiji MM, Qaqish RB. Synthesis of a fluorescent chitosan derivative and its application for the study of chitosan-mucin interactions. Carbohyd. Polym. 38: 99-107 (1999)
23. Garrett DA, Failla ML, Sarama RJ. Development of an *in vitro* digestion method to assess carotenoid bioavailability from meals. J. Agr. Food Chem. 47: 4301-4309 (1999)
24. Shim S, Kwon H. Assessing absorbability of bioactive components in aloe using *in vitro* digestion model with human intestinal cell. J. Food Biochem. 34: 425-438 (2010)
25. Bodmeier R, Chen H, Paeratakul O. A novel approach to the oral delivery of micro- or nanoparticles. Pharm. Res. 6: 413-417 (1989)
26. Huang M, Ma Z, Khor E, Lim LY. Uptake of FITC-chitosan nanoparticles by A549 cells. Pharm. Res. 19: 1488-1494 (2002)
27. Hong SS, Yoo HJ, Li H, Chung SJ, Kim DD, Shim CK. Effect of agitation on the *in vitro* permeability of xenobiotics across Caco-2 cell monolayers. J. Korean Pharm. Sci. 35: 111-116 (2005)
28. Lakeram M, Lockley DJ, Pendlington R, Forbes B. Optimisation of the Caco-2 permeability assay using experimental design methodology. Pharm. Res. 25: 1544-1551 (2008)
29. Guibal E, Milot C, Roussy J. Influence of hydrolysis mechanisms on molybdate sorption isotherms using chitosan. Separ. Sci. Technol. 35: 1021-1038 (2000)
30. Peng ZG, Hidajat K, Uddin MS. Adsorption of bovine serum albumin on nanosized magnetic particles. J. Colloid Interf. Sci. 271: 277-283 (2004)
31. Rezwan K, Studart A, Voros J, Gauckler L. Change of potential of biocompatible colloidal oxide particles upon adsorption of bovine serum albumin and lysozyme. J. Phys. Chem. B. 109: 14469-14474 (2005)
32. Vårum KM, Myhr MM, Hjerde RJN, Smidsrød O. *In vitro* degradation rates of partially *N*-acetylated chitosans in human serum. Carbohyd. Res. 299: 99-101 (1997)
33. Klockars M, Reitamo S. Tissue distribution of lysozyme in man. J. Histochem. Cytochem. 23: 932-940 (1975)

34. Mir MA. Lysozyme: A brief review. Postgrad. Med. J. 53: 257-259 (1977)
35. Peeters T, Vantrappen G. The paneth cell: A source of intestinal lysozyme. Gut 16: 553-558 (1975)
36. Ma Z, Yeoh HH, Lim LY. Formulation pH modulates the interaction of insulin with chitosan nanoparticles. J. Pharm. Sci. 91: 1396-1404 (2002)
37. Sadeghi AMM, Dorkoosh FA, Avadi MR, Weinhold M, Bayat A, Delie F, Gurny R, Larijani B, Rafiee-Tehrani M, Junginger HE. Permeation enhancer effect of chitosan and chitosan derivatives: Comparison of formulations as soluble polymers and nanoparticulate systems on insulin absorption in Caco-2 cells. Eur. J. Pharm. Biopharm. 70: 270-278 (2008)
38. Burton W, Nugent K, Slattery T, Summers B, Snyder L. Separation of proteins by reversed-phase high-performance liquid chromatography: I. Optimizing the column. J. Chromatogr. 443: 363-379 (1988)
39. Yoon JY, Kim JH, Kim WS. The relationship of interaction forces in the protein adsorption onto polymeric microspheres. Colloid. Surface A. 153: 413-419 (1999)